

enough conductivity for the STM experiments. Moreover, the dependence of the local surface conductivity on the individual hydrophilicity of the molecular groups located directly under the tip may provide new contrast mechanisms for the detection of individual segments in large molecules. Beyond these new possibilities for surface imaging and analysis, it may be possible to study the local properties of adsorbed water, especially those that are related to the mechanism of conductivity.

## REFERENCES AND NOTES

- R. Guckenberger, W. Wiegräbe, T. Hartmann, W. Baumeister, in *Scanning Tunneling Microscopy II*, R. Wiesendanger and H.-J. Güntherodt, Eds. (Springer, Berlin, 1992), pp. 52–98.
- O. Marti and M. Amrein, Eds., *STM and SFM in Biology* (Academic Press, San Diego, 1993).
- R. Guckenberger *et al.*, *Ultramicroscopy* **31**, 327 (1989).
- Z. Wang, T. Hartmann, W. Baumeister, R. Guckenberger, *Proc. Natl. Acad. Sci. U.S.A.* **87**, 9343 (1990).
- G. J. Leggett *et al.*, *J. Phys. Chem.* **97**, 8852 (1993).
- L. Gathercole, M. J. Miles, T. J. McMaster, D. F. Holmes, *J. Chem. Soc. Faraday Trans.* **89**, 2589 (1993).
- R. Guckenberger, F. Terán Arce, A. Hillebrand, T. Hartmann, *J. Vac. Sci. Technol. B* **12**, 1508 (1994).
- G. Cevc, *Biochim. Biophys. Acta* **1031–3**, 311 (1990).
- G. Cevc and A. A. Kornyshev, *J. Electroanal. Chem.* **330**, 407 (1992).
- J.-Y. Yuan, Z. Shao, C. Gao, *Phys. Rev. Lett.* **67**, 863 (1991).
- R. Guckenberger *et al.*, *Ultramicroscopy* **25**, 111 (1988).
- Input stage (20-gigohm feedback resistor) commercially available from Quintenz Hybridtechnik, Kramerstrasse 3, D-82061 Neuried, Germany.
- B. Hacker, A. Hillebrand, T. Hartmann, R. Guckenberger, *Ultramicroscopy* **42–44**, 1514 (1992).
- M. Heim, G. Cevc, R. Guckenberger, H. F. Knapp, in preparation.
- A. Schaper, L. I. Pietrasanta, T. M. Jovin, *Nucleic Acids Res.* **21**, 6004 (1993).
- R. Guckenberger *et al.*, in preparation.
- D. Beaglehole, E. Z. Radlinska, B. W. Ninham, H. K. Christenson, *Phys. Rev. Lett.* **66**, 2084 (1991).
- G. Cevc, in *Hydration of Biological Macromolecules*, E. Westhof, Ed. (Macmillan, New York, 1993), pp. 338–390.
- R. Guckenberger *et al.*, *J. Vac. Sci. Technol. B* **9**, 1227 (1991).
- D. B. Kell, *Bioelectrochem. Bioenerget.* **27**, 235 (1992).
- We thank A. Schaper for providing the pUC18 plasmid DNA and T. Hartmann and R. M. Glaeser for valuable discussions. This work was supported by the Deutsche Forschungsgemeinschaft (SFB-266).

5 July 1994; accepted 4 October 1994

## Atomic Control of the SrTiO<sub>3</sub> Crystal Surface

Masashi Kawasaki, Kazuhiro Takahashi, Tatsuro Maeda, Ryuta Tsuchiya, Makoto Shinohara, Osamu Ishiyama, Takuzo Yonezawa, Mamoru Yoshimoto, Hideomi Koinuma

The atomically smooth SrTiO<sub>3</sub> (100) with steps one unit cell in height was obtained by treating the crystal surface with a pH-controlled NH<sub>4</sub>F-HF solution. The homoepitaxy of SrTiO<sub>3</sub> film on the crystal surface proceeds in a perfect layer-by-layer mode as verified by reflection high-energy electron diffraction and atomic force microscopy. Ion scattering spectroscopy revealed that the TiO<sub>2</sub> atomic plane terminated the as-treated clean surface and that the terminating atomic layer could be tuned to the SrO atomic plane by homoepitaxial growth. This technology provides a well-defined substrate surface for atomically regulated epitaxial growth of such perovskite oxide films as YBa<sub>2</sub>Cu<sub>3</sub>O<sub>7-δ</sub>.

In spite of enormous efforts since the discovery (1) and thin-film preparation (2) of high-temperature (high-T<sub>c</sub>) superconducting oxides, nobody has succeeded in the preparation of high-T<sub>c</sub> Josephson tunnel junction, the key device for superconducting electronics. One of the primary reasons is the unavailability of a device-quality single-crystal substrate. In view of such short

coherence length of high-T<sub>c</sub> superconductors (roughly 0.3 to 2 nm), both of the superconducting (S) and insulating (I) layer surfaces in SIS tunnel junction must be regulated on an atomic scale. Overcoming this severe requirement will require a substrate with excellent lattice matching and an atomically regulated surface.

The commercially available single-crystal oxide wafers are prepared by so-called mechanochemical polishing with an alkaline solution containing colloidal silica particles. As an example, the atomic force microscopy (AFM) image of an SrTiO<sub>3</sub> wafer surface is depicted in Fig. 1A. The surface has a small corrugation of 0.2 to 0.8 nm and is as smooth as that of Si wafer without any special treatment. However, this surface was not sufficiently smooth for using atomic lay-

er epitaxy to deposit various oxide materials. Extensive studies on high-T<sub>c</sub> superconductors and related oxide thin films are now enabling atomic layer-by-layer growth of these films, as verified by the observation of intensity oscillations in reflection high-energy electron diffraction (RHEED) (3, 4). This technology is expected to explore a novel field of ceramics research because of its ability to artificially construct new compounds and devices (5). The substrate most frequently used is SrTiO<sub>3</sub>, and it must be clean and have an atomically smooth surface. The in situ cleaning procedures, such as heating in an oxygen flow (6), ion bombardment cleaning (7), and sublimation of a Bi film deposited on SrTiO<sub>3</sub> (8) were reported to be effective for the former purpose because carbon-containing impurities could be removed from the surface. However, these processes cannot improve the surface smoothness. Thus, the surface roughness shown in Fig. 1A must be overcome by a new method.

The crystal structure of SrTiO<sub>3</sub> is of the perovskite type and consists of alternating stacks of SrO and TiO<sub>2</sub> atomic layers. If one could find a wet solution that dissolves one of the atomic layers but not the other atomic layer, one should be able to prepare an atomically smooth surface terminated by the latter atomic layer. Because SrO is a basic oxide and TiO<sub>2</sub> is an acidic oxide, controlling the pH of the wet etch solution may accomplish this purpose.

Buffered NH<sub>4</sub>F-HF (BHF) solutions with various pH values were tested in this study. The NH<sub>4</sub>F concentration was kept at 10 M. The SrTiO<sub>3</sub> substrates with (100) polished planes were immersed in the BHF solutions for 10 min, rinsed with pure water and ethanol, and dried in a nitrogen stream. The AFM image taken in air for the substrate treated with a BHF (pH = 4.5) solution is shown in Fig. 1B. This image shows that the surface is composed of steps and atomically flat terraces. The step height was 0.4 nm, which corresponded to the unit cell length of SrTiO<sub>3</sub>. Such images were reproducibly observed on the entire surface of the substrates treated with BHF solutions (pH = 4.4 to 4.6). The ratio of the step height to the terrace width (150 nm) gives an off angle of 0.15°, which is in good agreement with the value determined by the x-ray diffraction. For the wafers treated by the BHF solutions with pH > 5, island-like residues of 0.2 to 0.4 nm in height were observed on the terraces. By treating the wafer in solutions with pH < 4, surfaces similar to that shown in Fig. 1B were obtained, but square etch pits were present. We presume that crystal defects and polishing damage are responsible for the etch pits.

The atomic smoothness of the substrate surface treated with BHF (pH = 4.5) was

M. Kawasaki, PRESTO, JRDC, and Research Laboratory of Engineering Materials, Tokyo Institute of Technology, Nagatsuta, Midori, Yokohama, 226 Japan.

K. Takahashi and T. Yonezawa, Shinkosha Co., Ltd., Sakae-ku, Yokohama, 247 Japan.

T. Maeda, R. Tsuchiya, M. Yoshimoto, H. Koinuma, Research Laboratory of Engineering Materials, Tokyo Institute of Technology, Nagatsuta, Midori, Yokohama, 227 Japan.

M. Shinohara and O. Ishiyama, Keihanna Research Laboratory, Shimazu Corp., Sorakugun, Kyoto 619-02, Japan.

further confirmed by RHEED. In this experiment, the substrate with the steps nearly parallel to the [010] direction was selected so that the electron beam azimuth was set parallel to the steps. The RHEED pattern of the BHF-treated substrate is shown in Fig. 2. The fine spots were observed on the zeroth and first Laue circles. Commercially supplied substrates always exhibited a streaky pattern rather than spots on the zeroth Laue circles. When the incident azimuth angle was set to the [001] direction (crossing the steps) on the same substrate, the streaky pattern was obtained, indicating that 0.4-nm-high steps are rough enough to diffuse the spots into streaks.

Because the step height corresponds to

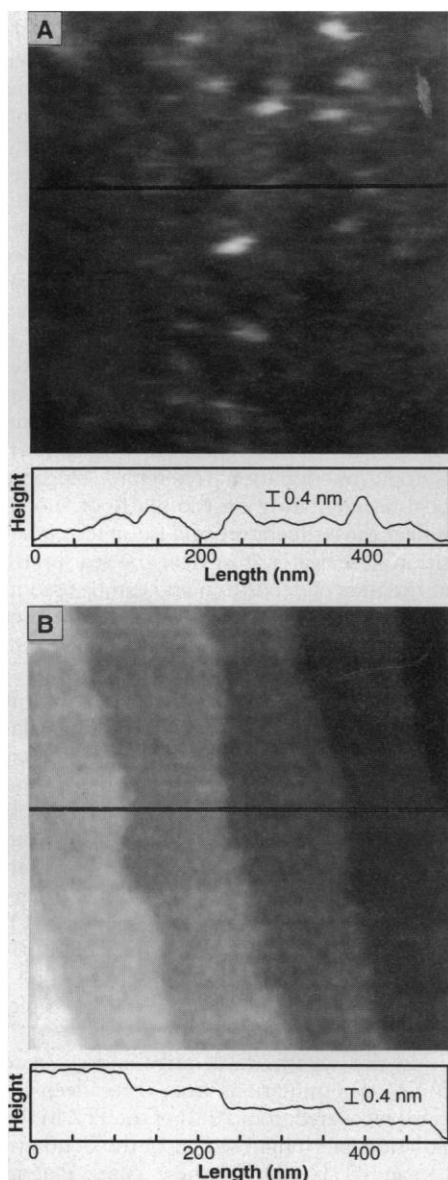


**Fig. 1.** AFM images of (A) commercial and (B) BHF-treated SrTiO<sub>3</sub> substrates. The vertical profile was taken along the line indicated in the image. The BHF-treated substrate exhibited atomically flat terraces and 0.4-nm-high steps.

the unit cell composed of SrO and TiO<sub>2</sub> atomic layers, the entire surface must be terminated by either one of the atomic layers. For elucidating the terminating atomic layer, low energy ion scattering spectroscopy (ISS) was carried out. The ion scattering spectra with an incident He ion (3 keV) angle set to [111] direction are shown in Fig. 3. Spectrum A revealed that the terminating atomic layer was TiO<sub>2</sub> with a coverage factor of 100% for a BHF-treated substrate. Commercially available substrates gave about 5 to 25% SrO termination and 95 to 75% TiO<sub>2</sub> termination (9, 10). Thus, the BHF solution selectively dissolves the SrO atomic plane to form an atomically smooth surface terminated by the TiO<sub>2</sub> atomic plane. Previously we suggested that the topmost atomic layer alternates from TiO<sub>2</sub> to SrO during the laser molecular beam epitaxy (MBE) growth of SrTiO<sub>3</sub> (11). This result was confirmed by the ISS measurement as shown in Fig. 3B (9). Thus, we can control the surface terminating atomic layer, TiO<sub>2</sub> or SrO, by the selective surface etching and homoepitaxial growth of SrTiO<sub>3</sub> film by laser MBE.

The cleaned SrTiO<sub>3</sub> (100) substrates were used for laser MBE growth of perovskite-type oxide films. A pulsed laser beam was focused on a single crystal or sintered ceramic target, and evaporated materials were deposited on the heated substrate (3).

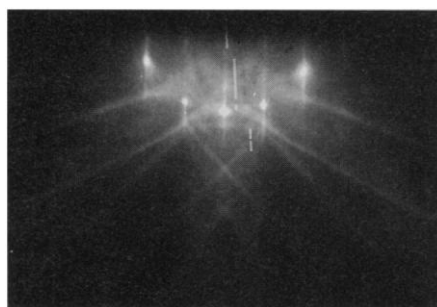


**Fig. 2.** The RHEED pattern of BHF-treated SrTiO<sub>3</sub> substrate with an azimuth of [010] direction (parallel to the steps). Fine spots rather than streaks were observed on the zeroth Laue circle.

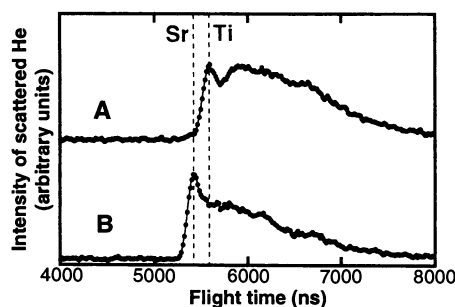


**Fig. 3.** Ion scattering spectra for (A) a BHF-treated substrate surface and (B) for a homoepitaxially grown film surface.

The intensity of the specular spot of the RHEED pattern was in situ-monitored during the film deposition. The RHEED signal variation during the homoepitaxy of SrTiO<sub>3</sub> in 10<sup>-6</sup> torr of oxygen on commercial and BHF-treated SrTiO<sub>3</sub> substrates at 630°C is shown in Fig. 4. In both curves A and B,

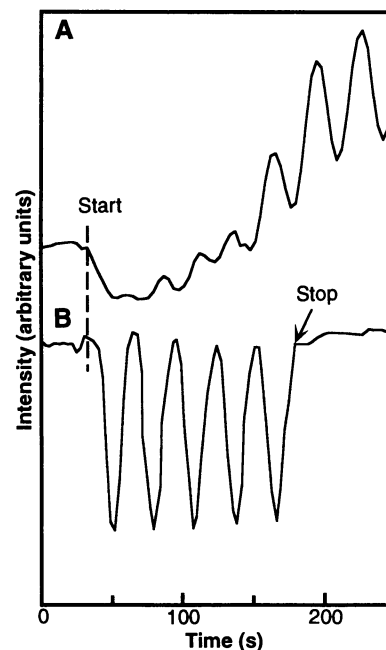


**Fig. 4.** The RHEED intensity variation during homoepitaxial growth of SrTiO<sub>3</sub> by laser MBE (A) on the commercial SrTiO<sub>3</sub> and (B) on the BHF-treated SrTiO<sub>3</sub>.

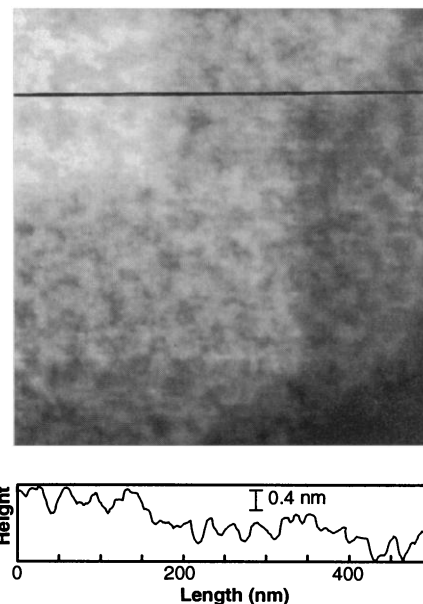


**Fig. 5.** An AFM image of the homoepitaxially grown SrTiO<sub>3</sub> film quenched at the bottom of the RHEED oscillation. The vertical profile was taken along the line indicated in the image. Islands 0.4 nm in height were randomly distributed on the atomically flat terraces.

clear oscillations were observed, indicating a two-dimensional layer-by-layer growth mode. On the BHF-treated substrate (curve B), the oscillation was quite regular and the signal intensity recovered to the value of the original surface at each peak. The oscillation persisted more than 300 cycles. This film exhibited a terraced surface in the AFM image similar to that of Fig. 1B. The AFM image in Fig. 5 represents the surface of the film quenched at the bottom of the RHEED oscillation. The film surface showed 0.4-nm-high islands randomly distributed on the atomically flat terraces. The film surface quenched at the peak of the RHEED oscillation showed the atomically flat surface similar to Fig. 1B. These results demonstrate that the RHEED oscillation during homoepitaxy of SrTiO<sub>3</sub> indeed originates from the oscillation of the atomic scale surface roughness due to the two-dimensional layer-by-layer growth. When the film was deposited at temperatures higher than 780°C, the homoepitaxy proceeds in a step-flow mode, in which the RHEED signal did not oscillate, but the film surface was well terraced on an atomic scale. The film growth on the commercial substrates did not show any step structures and gave rapidly damping RHEED oscillations (12).

For further examining the applicability of the BHF-treated substrates, such perovskite-type materials as PrGaO<sub>3</sub> and BaTiO<sub>3</sub> were heteroepitaxially grown by laser MBE to give a clear RHEED oscillation and atomically flat and well-terraced surfaces. When YBa<sub>2</sub>Cu<sub>3</sub>O<sub>7-8</sub> was grown on this terraced clean substrate, the film surfaces exhibited terraces and steps one unit cell in height aligned in one direction. Such results could not be obtained for the films deposited on the commercial substrates (13, 14). Thus, the BHF-treated substrates enable atomically regulated epitaxy of oxides comparable to that of semiconductors.

## REFERENCES

1. J. G. Bednorz and K. A. Müller, *Z. Phys. B*, **64**, 189 (1986).
2. H. Koinuma *et al.*, *J. Appl. Phys.* **62**, 1524 (1987).
3. H. Koinuma, H. Nagata, T. Tsukahara, S. Gonda, M. Yoshimoto, *Appl. Phys. Lett.* **58**, 2027 (1991).
4. T. Terashima *et al.*, *Phys. Rev. Lett.* **65**, 2684 (1991).
5. See, for example, H. Koinuma, *Mater. Res. Soc. Bull.* **19**, 21 (September 1994).
6. M. Yoshimoto, H. Ohkubo, N. Kanda, H. Koinuma, *Jpn. J. Appl. Phys.* **31**, 3664 (1992).
7. T. Terashima *et al.*, *ibid.* **28**, L987 (1989).
8. S. Watanabe, T. Hikita, M. Kawai, *J. Vac. Sci. Technol.* **A9**, 2394 (1991).
9. M. Yoshimoto *et al.*, *Mater. Res. Soc. Symp. Proc.* **341**, 133 (1994).
10. M. Kawai *et al.*, *Appl. Surf. Sci.*, in press.
11. S. Gonda, H. Nagata, M. Kawasaki, M. Yoshimoto, H. Koinuma, *Physica* **C216**, 160 (1993).
12. M. Yoshimoto *et al.*, *Appl. Phys. Lett.* **61**, 2659 (1992).
13. J. P. Gong *et al.*, *Jpn. J. Appl. Phys.* **32**, L687 (1993).
14. M. Kawasaki *et al.*, *ibid.*, p. 1612.

22 August 1994; accepted 12 October 1994

# Meltwater Input to the Southern Ocean During the Last Glacial Maximum

Aldo Shemesh, Lloyd H. Burckle, James D. Hays

Three records of oxygen isotopes in biogenic silica from deep-sea sediment cores from the Atlantic and Indian sectors of the Southern Ocean reveal the presence of isotopically depleted diatomaceous opal in sediment from the last glacial maximum. This depletion is attributed to the presence of lids of meltwater that mixed with surface water along certain trajectories in the Southern Ocean. An increase in the drainage from Antarctica or extensive northward transport of icebergs are among the main mechanisms that could have produced the increase in meltwater input to the glacial Southern Ocean. Similar isotopic trends were observed in older climatic cycles at the same cores.

During the past three decades, some of the most fundamental observations regarding past climate change and the changing chemical properties of seawater have been based on oxygen isotope analyses of calcium carbonate shells of foraminifera (1–3). Questions of importance to paleoclimatology and paleoceanography—on such topics as ice volume changes, the temporal and spatial distribution of meltwater pulses, and the tempo and mode of glacial-interglacial climate change—have been successfully addressed. Disintegration of major continental ice sheets and the consequent occurrence of large meltwater plumes during Northern Hemisphere deglaciation were inferred from  $\delta^{18}\text{O}$  records from continental margin sediments (4–7) and sea level changes (8). All major meltwater discharge pulses into the Gulf of Mexico and other Northern Hemisphere regions (although not isochronous) are associated with deglaciation. These pulses have also imposed global changes in deep-water formation, in primary production, and in gas exchange between the ocean and the atmosphere. In the Southern Ocean, the presence of meltwater was inferred by indirect measurements of  $^{231}\text{Pa}/^{230}\text{Th}$  in sediments and paleonitrate proxies (9) and also by a combination of foraminiferal  $\delta^{18}\text{O}$  and diatom transfer functions (uncorrected for dissolution effects) in the Indian sector (10).

Although isotopic determination of foraminiferal calcium carbonate is applicable in marine sediments from low and mid-latitudes, it frequently has only marginal application in high-latitude regions such as the Southern Ocean because foraminiferal carbonate is frequently absent or present only in low concentrations in such regions. Recently, the use of oxygen isotopes of biogenic opal ( $\delta^{18}\text{O}_{\text{Si}}$ ) secreted by marine dia-

toms was shown to provide paleoceanographic information that is complementary to that derived from foraminiferal  $\delta^{18}\text{O}$  (11, 12). Thus, the thermal history of the surface water of the Southern Ocean and meltwater input to this region can be identified and used to reconstruct ice dynamics around Antarctica. Because global climate change is the sum of local and regional climate change, the ability to recover oxygen isotope records from high southern latitudes provides a better understanding of global climate change.

South of the Polar Front zone (PFZ), diatoms are the dominant photosynthetic algae. They are light-limited, live within the uppermost layer of surface water, and secrete an opaline skeleton with known isotopic fractionation. Therefore, biogenic opal accumulating on the sea floor should reflect the temperature and isotopic composition of seawater at or near the sea surface at the time of deposition and can be used to reconstruct past variations in surface water properties. Earlier studies in sediments of the Weddell Sea and South Atlantic (12, 13) have shown that diatom  $\delta^{18}\text{O}$  records exhibit the predicted variation between glacial and interglacials. During glacial maxima, sea surface temperature is lower, and there is an increase in continental ice volume that preferentially removes  $^{16}\text{O}$  from the ocean. Therefore, the content of  $^{18}\text{O}$  in the solid phase in both foraminiferal carbonate and diatom opal is higher (1, 11). Global warming and the melting of continental ice during interglacials produces  $^{18}\text{O}$  minima in opal and carbonate during interglacials.

In this report, we describe and evaluate  $\delta^{18}\text{O}_{\text{Si}}$  determinations from three deep-sea cores recovered from south of the PFZ in the Atlantic and Indian sectors of the Southern Ocean (Table 1). In these cores, diatom samples from the last glacial maximum (LGM) (about 18,000 years ago) exhibit light  $\delta^{18}\text{O}_{\text{Si}}$  values; because temperatures should have been lower during the LGM, this result is contrary to the expectation that

A. Shemesh, Department of Environmental Sciences and Energy Research, The Weizmann Institute of Science, Rehovot, 76100, Israel.  
L. H. Burckle and J. D. Hays, Lamont-Doherty Earth Observatory of Columbia University, Palisades, NY 10964, USA.